

From the differential equation for  $W$

$$\dot{W} = S^T B B^T S; \quad W(t_f) = 0 \quad (31)$$

The solution is

$$w_{ij}(t) = 0 \quad \forall t; \quad i, j \neq 1 \quad (32)$$

$$w_{11}(t) = -\tau^2 \left\{ \tau/2 - \left[ \tau/2 e^{\frac{2(t-t_f)}{\tau}} - 2\tau e^{\frac{(t-t_f)}{\tau}} - 2\tau e^{\frac{(t-t_f)}{\tau}} \left( \frac{(t-t_f)}{\tau} - 1 \right) + (1/\tau)(t-t_f)^2 + (1/2\tau^2)(t-t_f)^3 + (t-t_f) \right] \right\} \quad (33)$$

And finally from the differential equation for  $M$

$$\dot{M} = -S^T C; \quad M(t_f) = 0 \quad (34)$$

One obtains the solution

$$m_2(t) = m_3(t) = 0 \quad (35)$$

$$m_1(t) = -\int_t^{t_f} (\xi - t_f) a_{T_n}(\xi) d\xi \quad (36)$$

With  $W(t)$  being singular, use of the term-by-term expansion of Eq. (21) rather than using Eq. (22) yields the solution for  $v$  as

$$v_2 = v_3 = 0 \quad (37)$$

$$v_1 = -\frac{1}{w_{11}(t)} \{x - \beta v + \tau^2(e^{\beta/\tau} - 1 - \beta/\tau) a_{m_n} + m_1\} \quad (38)$$

Where

$$\beta \triangleq (t - t_f)$$

The control, from Eq. (27), is then

$$u(t) = \frac{\Lambda}{(t_g)^2} \{x + t_g v + \tau^2(e^{-T} - 1 + T) a_{m_n} + m_1\} \quad (39)$$

where

$$t_g \triangleq -\beta = (t_f - t)$$

$$T \triangleq t_g/\tau$$

$$\Lambda \triangleq \frac{(e^{-T} - 1 + T)}{\left\{ \frac{1}{2T^2} e^{-2T} + \frac{2}{T} e^{-T} - \frac{T}{3} - \frac{1}{T} - \frac{1}{2T^2} + 1 \right\}} \quad (40)$$

#### Comparison of Results

By comparing the above guidance law with that derived by Cottrell for the nonmaneuvering target it is seen that the difference is an additional term  $(\Lambda m_1/t_g^2)$  for the present guidance law. If the target is undergoing an evasive maneuver of a constant  $g$  turn, then the target acceleration is constant in Eq. (36) and then Eq. (39) becomes

$$u(t) = \frac{\Lambda}{(t_g)^2} \left\{ x + t_g v + \tau^2(e^{-T} - 1 + T) a_{m_n} - \frac{(t_g)^2}{2} a_{T_n} \right\} \quad (41)$$

This agrees with the intuitive derivation of Cottrell.

#### Possible Applications

In a general problem one may not have knowledge of future target acceleration. However, in the problem of a missile intercepting another missile, called the target missile, which in turn is homing on a bomber, the target missile undergoes a sinusoidal acceleration profile due to its response to the scintillation noise phenomenon. Thus, the frequency and amplitude of the acceleration may be obtained by system analysis. The phase information may be obtained by measurements of the missile velocity. In a problem of an anti-ballistic missile intercepting a re-entry vehicle (RV) one has knowledge of the flight path of the RV and, thus, its acceleration profile. Similarly, in an anti-satellite missile the target acceleration is a known quantity. Thus, the result presented here which requires knowledge of future target acceleration may be quite useful in several scenarios.

#### Summary and Conclusions

This Note presents the analytic derivation of the optimal closed-loop guidance law for a finite-bandwidth missile intercepting a maneuvering target. The inclusion of a maneuvering target is the element which complicates the analytic development in that the system equations become nonhomogeneous. The analytic derivation for this nonhomogeneous case is given in this paper, and the resulting optimal guidance law agrees with the intuitive result determined by Cottrell under the assumption of a target undergoing a constant acceleration.

#### References

- <sup>1</sup> Cottrell, R. G., "Optimal Intercept Guidance for Short Range Tactical Missiles," *AIAA Journal*, Vol. 9, No. 7, July 1971, pp. 1414-1415.
- <sup>2</sup> Cottrell, R. G., "Optimal and Sub-Optimal Guidance Laws for Air-to-Air Interception," Interdepartmental Note, 2342.0520/114, Nov. 13, 1969, Hughes Aircraft Co., Culver City, Calif.
- <sup>3</sup> Bryson, A. E. and Ho, Y. C., *Applied Optimal Control*, Blaisdell, Waltham, Mass., 1968.

## Correlation of the Over-All Thermal Resistance of Metallic 0-Rings Contacting Two Cylinders

G. E. SCHNEIDER\* AND M. M. YOVANOVICH†  
University of Waterloo, Waterloo, Ontario, Canada

#### Nomenclature

- $A$  = heat flow area ( $\pi D^2/4$ )
- $C_1$  = correlation parameter, Eq. (5)
- $C_2$  = correlation parameter, Eq. (5)
- $C_3$  = correlation parameter, Eq. (7)
- $D_m$  = mean ring diameter
- $d_i$  = inside tube diameter
- $d_o$  = outside tube diameter
- $E$  = modulus of elasticity
- $F$  = total force on 0-ring
- $k$  = thermal conductivity
- $P^*$  = dimensionless load [ $F(1-v^2)/ED_m^2$ ]
- $Q$  = heat flow rate
- $R$  = thermal resistance
- $R^*$  = dimensionless thermal resistance ( $kD_m/R$ )
- $T$  = temperature
- $t$  = tube wall thickness ( $2t = d_o - d_i$ )
- $t^*$  = dimensionless wall thickness ( $2t/d_o$ )
- $\nu$  = Poisson's ratio

#### Subscripts

- 1, 2, 3 = cylinders 1 and 2, and 0-ring, respectively
- $o$  = over-all

#### Introduction

THIS Note considers the over-all resistance to heat transfer across a joint formed by solid or hollow metallic 0-rings in contact with smooth, flat ends of cylinders, Fig. 1. Such

Received October 9, 1973; revision received November 26, 1973. The authors thank the Canadian National Research Council for its financial support of this project.

Index categories: Spacecraft Temperature Control Systems; Heat Conduction; Thermal Modeling and Experimental Thermal Simulation.

\* Research Assistant, Thermal Engineering Group, Department of Mechanical Engineering.

† Professor of Mechanical Engineering. Member AIAA.

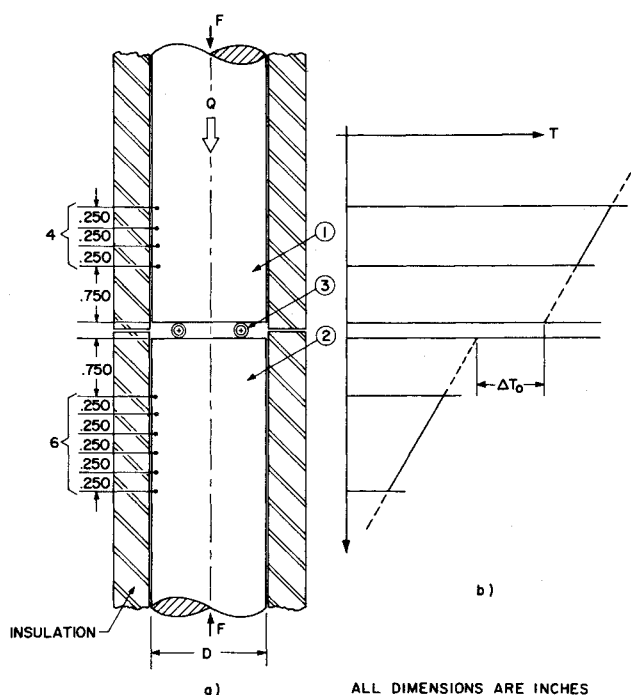


Fig. 1 Schematic of test apparatus with typical temperature distribution.

systems can be found in spacecraft thermal support applications where structural strength in addition to thermal insulating characteristics are required. Under vacuum conditions and negligible radiative heat transfer, all the heat must cross the joint by means of the O-ring, i.e., all the heat flowing in cylinder 1 is a) constricted as it enters the contact area between the O-ring and flat end, b) conducted through the walls of the O-ring, and c) made to experience a divergence of the heat flow lines as it enters cylinder 2. Thus, the over-all resistance consists of three resistances connected in series. If it were possible to predict the size of the contact area under normal loading, then one could, using existing thermal constriction resistance theories,<sup>1-5</sup> predict the over-all resistance. Unfortunately one is unable to predict the effect of loads upon the contact area of commercially available solid or hollow O-rings because they 1) do not lie flat under zero load, 2) are not smooth, and 3) undergo both elastic and plastic deformation under moderate loading.

This Note describes the O-rings, the experimental program followed to determine the over-all resistance, and the dimensionless groups used to correlate the test data.

#### System

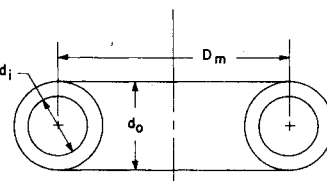
The solid and hollow metallic O-rings used in the experimental program are shown schematically in Fig. 2. The geometric, thermal, and physical characteristics of the nine different O-rings tested are given in Table 1.

Table 1 System parameters at 20°C.

$D_m$ (in.)	0.438	0.563	0.813
$d_o$ (in.)	0.062	0.062	0.062
$t$ (in.)	0.006 0.010 0.031	0.006 0.010 0.031	0.006 0.010 0.031
$k$ (Btu/hr-ft-°F) <sup>a</sup>	8.33	8.33	8.33
$E$ (psi)	$30 \times 10^6$	$30 \times 10^6$	$30 \times 10^6$
$\nu$	0.30	0.30	0.30

<sup>a</sup> Handbook of Chemistry and Physics, 53rd ed.

Fig. 2 O-ring geometric parameters.



The O-rings and the cylinders were fabricated from stainless steel: SS 321 and SS 304, respectively. The O-rings were drilled through to allow evacuation of the space within the ring as well as the region between the ring and the cylinders. The right circular cylinders were 1.50 in. diam.  $\times$  3.50 in. long. The test ends were first made flat, then polished to a roughness less than  $10\mu$  in rms. Four thermocouples were attached to cylinder 1 and six attached to cylinder 2, with spacings as shown in Fig. 1. All thermocouples were fabricated from copper-constantan wire.

#### Test Program

A total of nine different O-rings were tested. The system as shown in Fig. 1 was placed in a chamber and all tests were conducted in a vacuum ( $<10^{-5}$  mm Hg). A cartridge heater supplied heat to cylinder 1, and this heat was removed from the system by means of temperature controlled cool water in contact with cylinder 2. The heat input into the system was adjusted such that the temperature level at the joint did not result in an appreciable radiative effect. The system was well insulated to minimize heat losses to the surroundings. An axial load was applied to the system by means of a leverage system. By means of the mechanical advantage, the normal contact loads ranged from 200 to 1000 lbs. A strain gauge located above, but thermally insulated from, the heat source was used to monitor the contact load. Temperature measurements were made by means of 10 copper-constantan thermocouples. Only steady-state temperatures were recorded, and all measurements were made during the first loading cycle only.

At the conclusion of each test, the O-rings were examined and found to have experienced significant plastic deformation. The ends of the cylinders also exhibited plastic deformation in the region which had contacted the O-ring. The ends of the cylinders were surface ground flat and polished before they were used in subsequent tests with O-rings having identical mean diameters.

#### Test Results and Correlations

The test results consisted of the steady-state thermocouple measurements and the contact load. A computer program determined the extrapolated surface temperatures, the over-all temperature drop across the joint and the total heat flow rate. The experimentally determined over-all resistance is calculated by means of the following expression:

$$R_o = \Delta T_o / Q \quad (1)$$

where the total heat flow rate  $Q$  is determined from

$$Q = k_2 A (\Delta T / \Delta X)_2 \quad (2)$$

Both the thermal conductivity and the temperature gradient used in Eq. (2) were obtained for cylinder 2.

An analysis based upon the following assumptions: 1) the O-rings always contact the flats along the entire circumference, 2) the O-rings are smooth, 3) the deformation of the O-rings and the flats is elastic, and 4) the available thermal constriction theories are applicable, leads to two important dimensionless groups: thermal resistance number and contact load number.

The dimensionless over-all resistance number is defined as

$$R_o^* = k D_m R_o \quad (3)$$

while the dimensionless contact load number is defined as

$$P^* = F(1 - \nu^2) / E D_m^2 \quad (4)$$

**Table 2** Correlation parameters  $C_1$ ,  $C_2$ ,  $C_3$  and  $m$ 

0-ring		Correlation parameters			
$Dm$ (in.)	$t^*$	$C_1$	$C_2$	$C_3$	$m$
0.438	0.194	1.108	583.0	1300	0.470
0.438	0.323	1.034	770.7	1300	0.470
0.438	1.000	0.656	2236.7	1300	0.470
0.563	0.194	1.168	436.3	810	0.364
0.563	0.323	1.025	543.6	810	0.364
0.563	1.000	0.875	794.8	810	0.364
0.813	0.194	1.265	195.2	320	0.288
0.813	0.323	1.193	232.7	320	0.288
0.813	1.000	1.051	310.9	320	0.288

If one considers  $F/D_m^2$  to be an effective contact pressure, then  $P^*$  can be defined as the dimensionless contact pressure.

The two dimensionless groups defined by Eqs. (3) and (4) were used with the following expression:

$$R_o^* = C_1 \ln(C_2/10^6 P^*) \quad (5)$$

to correlate all the test data. The correlation parameters  $C_1$  and  $C_2$  were determined by means of curve fitting to have the values

**Table 3** Limits on the load parameter  $P^*$ 

$Dm$ (in.)	$t^*$	$P^*$	
		minimum	maximum
0.438	0.194	$50 \times 10^{-6}$	$170 \times 10^{-6}$
	0.323	$50 \times 10^{-6}$	$170 \times 10^{-6}$
	1.000	$50 \times 10^{-6}$	$170 \times 10^{-6}$
0.563	0.194	$20 \times 10^{-6}$	$100 \times 10^{-6}$
	0.323	$20 \times 10^{-6}$	$100 \times 10^{-6}$
	1.000	$30 \times 10^{-6}$	$100 \times 10^{-6}$
0.813	0.194	$10 \times 10^{-6}$	$50 \times 10^{-6}$
	0.323	$15 \times 10^{-6}$	$50 \times 10^{-6}$
	1.000	$15 \times 10^{-6}$	$50 \times 10^{-6}$

shown in Table 2. A further examination of the parameter  $C_2$  showed that it could also be correlated with a third dimensionless parameter

$$t^* = 2t/d_o \quad (6)$$

defined as the dimensionless tube wall thickness number.

A cross plot of  $C_2$  against  $t^*$  leads to the following relationship:

$$C_2 = C_3(t^*)^m \quad (7)$$

The values of the new correlation parameters  $C_3$  and  $m$  are also given in Table 2 for the nine 0-rings examined.

It was not possible to obtain a correlation of the parameter  $C_1$  against any of the characteristics of the 0-rings and the cylinders.

All the data obtained for the dimensionless pressures shown in Table 3 are correlated by means of Eqs. (5) and (7) with the values of  $C_1$ ,  $C_3$  and  $m$  given in Table 2 to within  $\pm 2\%$  for the solid 0-rings and those 0-rings having  $t^* = 0.323$ . For  $t^* = 0.194$ , all the data is correlated to  $\pm 3\%$ . The range of  $P^*$  could be extended if larger errors are acceptable.

### Conclusions

Based upon the results of the semi-empirical study, one can conclude that all the test data for the nine 0-rings tested can be correlated adequately using only three dimensionless numbers:  $R_o^*$ ,  $P^*$ ,  $t^*$ . These numbers were derived by means of an analysis based upon ideal conditions which are approximations for commercially available 0-rings.

### References

- Yovanovich, M. M., *Advanced Heat Conduction*, edited by C. L. Tien, Holt, Rinehart, and Winston, New York, to be published.
- Cooke, J. C., "Triple Integral Equations," *Quarterly Journal of Mechanics and Applied Mathematics*, Vol. 16, 1963, pp. 193-207.
- Smythe, W. R., "The Capacitance of a Circular Annulus," *Journal of Applied Physics*, Vol. 22, 1951, pp. 1499-1501.
- Yovanovich, M. M., "Thermal Conductance of a Row of Cylinders Contacting Two Planes," *Progress in Astronautics and Aeronautics*, Vol. 29, 1972, pp. 307-317.
- Yip, F. C., "Thermal Contact-Constriction Resistance," PhD thesis, 1969, Department of Mechanical Engineering, University of Calgary, Calgary, Alberta, Canada.